Imaging of Adrenal Incidentalomas with PET Using ^{11}C-Metomidate and ^{18}F-FDG

Heikki Minn, MD[1,2]; Anna Salonen, BSc[1]; Johan Friberg, MD[1]; Anne Roivainen, PhD[1]; Tapio Viljanen, MSc[1]; Jaakko Långsjö, MD[1]; Jorma Salmi, MD[3]; Matti Välimäki, MD[4]; Kjell Någren, PhD[1]; and Pirjo Nuutila, MD[1,5]

[1]Turku PET Centre, University of Turku, Turku, Finland; [2]Department of Oncology and Radiotherapy, Turku University Central Hospital, Turku, Finland; [3]Department of Internal Medicine, Tampere University Hospital, Tampere, Finland; [4]Department of Internal Medicine, Helsinki University Hospital, Helsinki, Finland; and [5]Department of Internal Medicine, Turku University Central Hospital, Turku, Finland

Our aim was to evaluate the use of PET with ^{11}C-metomidate and ^{18}F-FDG for the diagnosis of adrenal incidentalomas. **Methods:** Twenty-one patients underwent hormonal screening before dynamic imaging of the upper abdomen with ^{11}C-metomidate, and for 19 of these 21 patients, static ^{18}F-FDG imaging followed. Uptake of ^{11}C-metomidate and ^{18}F-FDG in incidentalomas was quantified and correlated with the hormonal work-up and the mass size on CT (median, 2.5 cm; range, 2–10 cm). **Results:** The final diagnoses were hormonally active adenoma (n = 7), nonsecretory adenoma (n = 5), adrenocortical carcinoma (n = 1), pheochromocytoma (n = 2), benign noncortical tumor (n = 2), normal adrenal (n = 1), and malignant noncortical tumor (n = 3). Diagnosis was established at surgery (n = 9), percutaneous biopsy (n = 4), or follow-up (n = 8). The highest uptake of ^{11}C-metomidate, expressed as standardized uptake value (SUV), was found in adrenocortical carcinoma (SUV = 28.0), followed by active adenomas (median SUV = 12.7), nonsecretory adenomas (median SUV = 12.2), and noncortical tumors (median SUV = 5.7). Patients with adenomas had significantly higher tumor–to–normal-adrenal ^{11}C-metomidate SUV ratios than did patients with noncortical tumors. ^{18}F-FDG detected 2 of 3 noncortical malignancies but failed to detect adrenal metastases from renal cell carcinoma. All inactive and most active adenomas were difficult to detect with ^{18}F-FDG against background activity, whereas both pheochromocytomas and adrenocortical carcinoma showed slightly increased uptake of ^{18}F-FDG. There was no correlation between uptake of ^{11}C-metomidate or ^{18}F-FDG and mass size. **Conclusion:** ^{11}C-Metomidate is a promising PET tracer to identify incidentalomas of adrenocortical origin. ^{18}F-FDG should be reserved for patients with a moderate to high likelihood of neoplastic disease.

Key Words: adrenal gland; PET; radionuclide imaging; metomidate; ^{18}F-FDG

J Nucl Med 2004; 45:972–979

The rate of finding unexpected adrenal masses, so-called incidentalomas, has been increasing because of increased use of CT, MRI, and ultrasound to study symptoms potentially originating from the abdomen (*1*). Patients with incidentalomas are subjected to hormonal screening and, sometimes, an extensive diagnostic work-up, especially if malignancy is suspected (*2*). Patients with a history of oncologic disease clearly have a high risk (32%–75%) for adrenal metastasis (*2–4*), and adrenocortical adenoma accounts for 36%–94% of incidentalomas diagnosed in patients without a history of cancer (*1,2,5*). Other final diagnoses for incidentalomas include pheochromocytomas, lipomas, cysts, or false adrenal masses actually arising from a nearby organ such as the liver, kidney, or stomach (*1,2*).

Adrenal tumors are found incidentally in up to 5% of patients, illustrating the need for an effective strategy to determine whether a patient should be treated surgically, pharmacologically, or not at all (*1,2*). Besides clinical history and hormonal profile, mass size and imaging characteristics play an important role in the diagnostic algorithm, which by no means has matured to a universally approved form (*6*). In some patients, the size, morphologic appearance, attenuation on CT, and growth pattern of the adrenal mass do not disclose its nature. A positive intracellular lipid signal on MRI suggests a benign adenoma, but in the absence of characteristic features on MRI or CT, functional imaging with radionuclides should be considered for differential diagnosis (*7,8*).

Recently, PET using ^{11}C-labeled metomidate was introduced for the identification of indeterminate adrenal masses (*9,10*). Metomidate is an inhibitor of 11β-hydroxylase, a key enzyme in the biosynthesis of cortisol and aldosterone by the adrenal cortex. Our goal was to evaluate ^{11}C-metomidate PET in the diagnosis of incidentalomas and to study whether uptake of tracer is associated with adrenal cortex function.

MATERIALS AND METHODS

Patients

Twenty-one patients (14 female, 7 male) aged 21–79 y participated in the study. Written informed consent to undergo PET

Received Oct. 20, 2003; revision accepted Dec. 29, 2003.

For correspondence or reprints contact: Heikki Minn, MD, Department of Oncology and Radiotherapy, Turku University Central Hospital, P.O. Box 52, FIN-20521 Turku, Finland.

E-mail: heikki.minn@utu.fi

imaging was obtained from all patients, and the consent form and study protocol were approved by the Ethical Committee of the Local Hospital District. Pertinent clinical characteristics of the patients and their final diagnoses after PET are given in Table 1. The patients were referred by a certified specialist in either clinical endocrinology or oncology because of unilateral (n = 19) or bilateral (n = 2, patients 19 and 21) adrenal masses incidentally discovered during an abdominal imaging procedure (ultrasound or CT). The axial diameter of the mass was required to be at least 2 cm in one direction, and all patients with clear evidence of hormonally active tumor were excluded. Patient 7 had previously undergone a left adrenalectomy because of hormonally silent adenoma, and 6 patients had a history of malignancy without evidence of recurrence or metastatic disease.

All patients whose incidentaloma was found at ultrasound also underwent abdominal CT, which served as a morphologic gold standard for measurement of lesions. The median diameter at CT was 2.5 cm (range, 2–10 cm). Before imaging, the patients underwent hormonal evaluation including serum cortisol, plasma adrenocorticotropic hormone, plasma renin, serum aldosterone, serum sodium and potassium, serum dehydroepiandrosterone sulfate, plasma glucose, and 24-h urine metanephrine and normetanephrine. An overnight oral 1-mg dexamethasone suppression test was performed to assess adrenocortical hormonal activity in all but 3 patients (patients 8, 14, and 19). This study was part of a larger multicenter trial performed under European Cooperation in the Field of Scientific and Technical Research (COST) action B12.

Synthesis of Radiopharmaceuticals

^{11}C-Metomidate was prepared by a modification of the published procedure (*9*). ^{11}C-Methyl triflate, prepared by a standard procedure (*11*), was trapped at 0°C in 100 mL of acetone containing 0.5–1.0 mg of *O*-desmethyl precursor (R028141; Janssen Research Foundation) and 2.0–4.0 mL of freshly prepared tetrabutylammonium hydroxide (1 mol/L, aqueous). When trapping was completed, the reaction mixture was purified on a μBondapak C-18 column (125Å, 10 μm, 7.8 × 300 mm in internal diameter; Waters) using an eluent of methanol:water, 60:40, and a flow of 4 mL/min. The purified product was collected in a vessel containing 0.8 mL of sterile propylene glycol:ethanol, 7:3, evaporated, redissolved in sterile phosphate buffer (0.1 mol/L, pH 7.4), and filtered through a Gelman Acrodisc sterile filter (PN 4192, 0.2 mm; Pall Corp.). The final radiochemical yield of ^{11}C-metomidate from ^{11}C-methyl triflate was 40%–80%, with a specific radioactivity of 60 ± 20 GBq/μmol. The radiochemical purity was higher than 98% and stable for at least 2 h. Omission of propylene glycol and ethanol during evaporation decreased radiochemical purity (80%–90%), showing that the radiochemical impurities were formed by radiolysis.

TABLE 1
Patient Characteristics, Final Diagnosis, and PET Findings Expressed as SUV of the Adrenal Mass

Patient characteristic								PET findings (SUV)	
Patient no.	Sex	Age (y)	Previous malignancy	Oral dexamethasone test	Mass diameter (cm) on CT	Final diagnosis	Operation	^{11}C-MTO	^{18}F-FDG
1	F	57	Uterine cancer	Positive	2.5	Adenoma, active	Yes	20.9	2.2
2	F	59	None	Positive	3	Adenoma, active	Yes	11.9	3.9
3	F	74	Laryngeal cancer	Positive	2.5	Adenoma, active	No*	26.1	2.5
4	M	67	None	Positive	2.6	Adenoma, active	No*	12.7	1.8
5	F	68	None	Positive	4	Adenoma, active	No*	9.1	1.8
6	F	48	None	Positive	2	Adenoma, active	Yes	16.0	3.4
7	F	74	Colorectal cancer Renal cell cancer	Positive	2.5	Adenoma, active	No*	10.2	2.3
8	F	59	None	Not done	2	Adenoma, inactive	No	12.2	1.6
9	M	66	Colorectal cancer	Negative	2	Adenoma, inactive	No†	10.0	1.7
10	M	55	None	Negative	3	Adenoma, inactive	Yes	25.4	Not done
11	M	54	None	Negative	2.5	Adenoma, inactive	Yes	16.2	1.7
12	M	63	None	Negative	2	Adenoma, inactive	No	7.8	Not done
13	F	34	None	Negative	4.8	Adrenocortical cancer	Yes	28.0	2.9
14	F	43	None	Not done	2	Normal adrenal	No	11.3	1.7
15	F	21	None	Negative	7	Cyst	No‡	1.2	0.5
16	F	55	None	Negative	2	Lipoma	No§	13.3	2.2
17	F	41	None	Negative	2.5	Pheochromocytoma	Yes	10.5	3.0
18	F	67	None	Negative	4	Pheochromocytoma	Yes	7.8	2.9
19	M	69	Renal cell cancer	Not done	3	Metastasis	No‡	2.0	1.7
20	M	71	Prostate cancer	Negative	6	Hepatocellular cancer	Yes	6.2	8.3
21	F	79	None	Positive	10	Lymphoma	No†	2.3	16.4

*Operation withheld because of intercurrent morbidity.
†Core biopsy without adrenalectomy.
‡Fine-needle biopsy.
§CT findings consistent with lipoma.
MTO = metomidate.

The synthesis of ^{18}F-FDG followed a previously described nucleophilic substitution procedure (*12*). The radiochemical purity of ^{18}F-FDG was at least 95%, and the specific radioactivity at the end of synthesis was more than 75 GBq/μmol.

Patient Preparation

^{11}C-Metomidate and ^{18}F-FDG PET studies were performed either on the same day or within 1 wk of each other. For both PET studies, the subjects fasted at least 6 h or overnight. Drinking of water was allowed ad libitum. Before ^{11}C-metomidate PET a 2-wk break was required from drugs that could affect uptake of tracer (ketoconazole, metyrapone). For the ^{11}C-metomidate study, 2 catheters were inserted in contralateral forearm veins to inject tracer and to draw blood samples during imaging. The blood-sampling arm was wrapped in an electric blanket to heat the arm for arterialization of blood samples. The subject was placed supine in the PET scanner with the arms held upright, and correct positioning to image the adrenals was secured with anatomic landmarks and CT images. For repositioning during the second PET study, laser lines were marked on the skin with a felt-tip pen. At least 3 h separated injection of the 2 radiopharmaceuticals, with ^{11}C-metomidate always preceding ^{18}F-FDG. Two patients (patients 10 and 12) did not undergo ^{18}F-FDG imaging for logistic reasons.

Image Acquisition and Processing

An 18-ring 2-dimensional whole-body PET scanner (Advance; General Electric Medical Systems) operated in 2-dimensional mode was used. The camera has bismuth germanate detectors, which image 35 planes at 4.25-mm intervals in a single session. The diameter of the field of view is 55 cm, and the axial length is 15.2 cm. Both PET studies were corrected for photon attenuation with 10- to 12-min preinjection transmission scans using robotically operated rods containing ^{68}Ge/^{68}Ga. For cases in which ^{18}F-FDG imaging was performed in whole-body mode, 2-min postemission transmission scans were obtained.

Dynamic imaging was started by bolus intravenous injection of a median dose of 432 MBq (range, 211–444 MBq) of ^{11}C-metomidate, and a 45-min emission scan was subsequently acquired (frame rate of 5 × 60 s, 5 × 180 s, 3 × 300 s, and 1 × 600 s). Arterialized venous blood was frequently sampled for measurement of radioactivity throughout imaging and determination of metabolites of ^{11}C-metomidate. Samples for the latter were obtained at 2, 6, 10, 20, 30, and 40 min after injection of tracer. ^{18}F-FDG imaging ($n = 11$) was performed in steady state starting 45 min after intravenous injection and consisted of two 10-min frames. Alternatively, whole-body scans ($n = 8$) were obtained in the craniocaudal direction with 6–7 bed positions, each lasting 5 min. No blood samples were taken during ^{18}F-FDG imaging except for plasma glucose before tracer injection. The median dose of ^{18}F-FDG was 369 MBq (range, 251–378 MBq). All image acquisition data were corrected for dead time, decay, and photon attenuation and reconstructed with an ordered-subsets expectation maximization algorithm using 4 iterations. The final in-plane spatial resolution in reconstructed images was 5 mm, and the axial resolution was 6 mm.

Blood Metabolite Analysis

Venous blood samples were collected into heparinized tubes at 2, 6, 10, 20, 30, and 40 min after injection to measure the amount of unchanged ^{11}C-metomidate and radioactive metabolites in plasma. Plasma proteins were precipitated with acetonitrile, and the supernatant obtained after centrifugation was analyzed with high-performance liquid chromatography (HPLC) using a μBondapak C-18 reversed-phase column (125Å, 10 μm, 7.8 × 300 mm in internal diameter; Waters) at a flow rate of 6.0 mL/min and a gradient of 100% acetonitrile (B) in 50 mmol of phosphoric acid per liter (A) as follows: 0 min of 75% A and 25% B, 5.5 min of 40% A and 60% B, 7.5 min of 40% A and 60% B, and 8.5–9 min of 75% A and 25% B. A LaChrom HPLC system (Hitachi/Merck) and a Radiomatic 150TR radioactivity detector (Packard) were used.

Measurement of ^{11}C-Metomidate and ^{18}F-FDG Uptake

The adrenals were invariably seen as hot spots in the final ^{11}C-metomidate PET frame, which was used for defining regions of interest (ROI). Trace ROI function was used to outline ROIs encompassing the whole hot spot area in normal and enlarged adrenal glands, and mean (not maximum) radioactivity in the 3 consecutive axial planes with the highest radioactivity was used for further calculations. Similarly, a standard-sized circular ROI approximately 3 cm in diameter was drawn in 3 consecutive planes in the right lobe of the liver, also an organ with high uptake of ^{11}C-metomidate (*10*). In the kinetic analysis, the input function for uptake of ^{11}C-metomidate was corrected for 2 major labeled metabolites that constituted a variable but highly significant fraction of total plasma radioactivity. The corrected plasma and tissue time–activity curves derived from ROIs as explained above were used to calculate kinetic influx constant (K_i) values by applying the graphical analysis first described by Patlak (*13*). Standardized uptake values (SUVs) were also defined from the last frame, between 35 and 45 min, correcting tissue radioactivity for patient weight and injected dose (*14*).

Because normal adrenals have faint uptake of ^{18}F-FDG, definition of ROIs was much more difficult on ^{18}F-FDG PET images than on ^{11}C-metomidate PET images. Accordingly, we outlined ROIs onto ^{18}F-FDG planes by reading ^{18}F-FDG and ^{11}C-metomidate axial images together and by relating findings to those on corresponding CT scans. This was facilitated by the normal ^{18}F-FDG uptake seen in liver, spleen, kidneys, and, variably, in stomach and bowel. The second of the 2 time frames (55–65 min) was used for calculation of SUV in adrenals and liver, again using the mean value over 3 consecutive planes. For whole-body ^{18}F-FDG studies, only one 5-min frame was available for SUV calculation.

Statistical Analysis

Commercially obtained software (SPSS, release 11.0.1, standard version; SPSS Inc.) for Windows (Microsoft) was used for statistical evaluation. Results are expressed mostly as median and range. Normality of quantitative data was assessed with the Kolmogorov–Smirnov test. For normally distributed data, ANOVA and the independent-samples *t* test was used; for other data, nonparametric methods (the Kruskal–Wallis test and Mann–Whitney *U* test) were applied. The association between K_i and SUV was evaluated with the Pearson correlation coefficient. All *P* values are 2 tailed.

RESULTS

Final Diagnosis of Incidentalomas

The final diagnoses of 21 patients included 7 active adenomas as evidenced by a deficient dexamethasone sup-

pression test, 5 inactive adenomas, 1 adrenocortical carcinoma, 2 pheochromocytomas, 1 cyst, 1 lipoma, 1 normal adrenal falsely interpreted as tumor, and 3 noncortical malignancies (Table 1). Of the patients with active adenomas, 3 of 7 (43%) underwent adrenalectomy, whereas operation was withheld from the remaining 4 because of intercurrent disease ($n = 3$) or unexpected death due to coronary artery disease ($n = 1$). Diagnosis was confirmed histologically or cytologically for 13 patients and, for the remaining 8 patients, by characteristic radiologic appearance combined with concordant hormonal blood test findings and follow-up lasting a median of 14 mo (range, 9–21 mo). Patient 20 had well-differentiated hepatocellular carcinoma presenting as a pseudoadrenal mass (*1*).

Quantification of ^{11}C-Metomidate Uptake

Identification of adrenocortical adenomas and normal adrenal glands was easy with ^{11}C-metomidate PET because of the invariably high uptake of tracer in target organs with functional steroid hormone synthesis. In accordance with Bergström et al. (*10*), liver and, more variably, stomach and duodenum also showed moderate to high ^{11}C-metomidate uptake, which did not interfere with radioactivity seen in adrenal tissues in late images. PET images of 4 patients with different types of adrenal incidentalomas are shown in Figure 1.

Two major ^{11}C-metomidate polar metabolites with retention times of 2.3 and 3.2 min were seen in venous plasma with HPLC, and the rate of their appearance varied considerably between individual patients (Fig. 2). As a result, unchanged ^{11}C-metomidate accounted for a median of 28% (range, 17%–40%; $n = 12$) of total radioactivity at 40 min from injection, and the respective figure at 20 min was 40% (range, 22%–54%; $n = 12$). Figure 3A shows the time course of radioactivity in uncorrected and corrected plasma samples and selected tissues in a representative patient with adrenocortical adenoma. The HPLC analysis made clear that only plasma corrected for metabolites could be used as input when applying the graphical method to evaluate the rate of ^{11}C-metomidate uptake and metabolism in tissues. With the corrected input function, excellent fits were found for adrenal tumors and glands and for liver (Fig. 3B). A strong relationship between average SUV and graphical K_i was seen for all tumor types and normal adrenal glands ($r^2 = 0.73$, $P < 0.0001$).

In quantitative analysis, the highest ^{11}C-metomidate uptake among all tumors was seen in the single case of adrenocortical carcinoma, with an average SUV of 28.0 (Figs. 1E and 1F). This was followed in decreasing order of ^{11}C-metomidate uptake, expressed as average SUV, by active adenomas (median SUV = 12.7; range, 9.1–26.1; $n =$

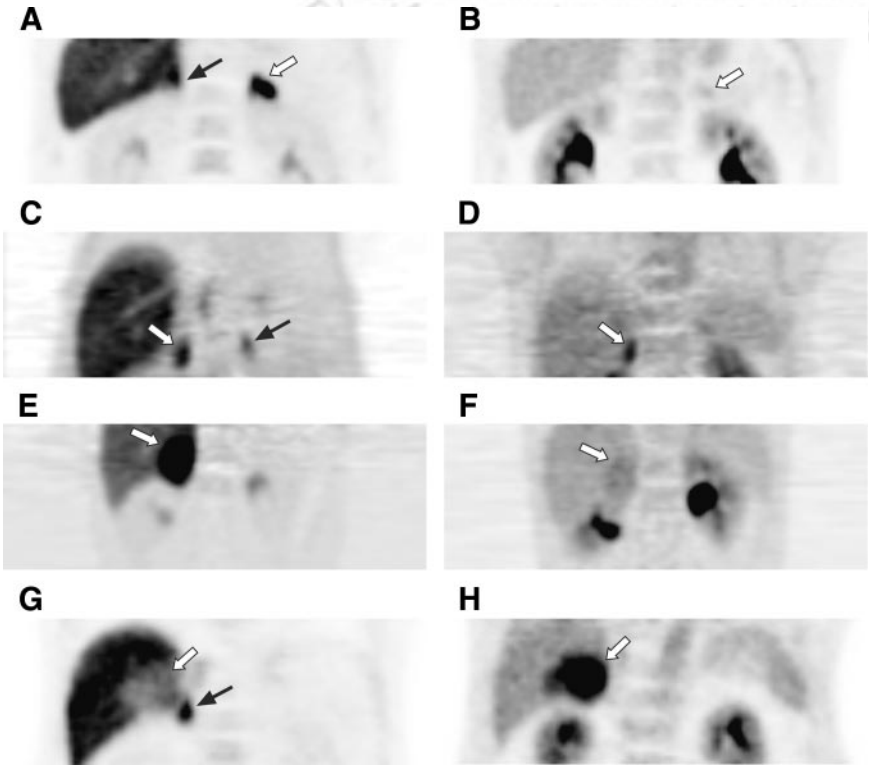

FIGURE 1. ^{11}C-Metomidate (left column) and ^{18}F-FDG (right column) PET images of patients with adrenal incidentalomas: a left-sided hormonally inactive adenoma (patient 11) (A and B), a right-sided cortisol-secreting adenoma (patient 2) (C and D), a right-sided adrenocortical carcinoma (patient 13) (E and F), and a right-sided hepatocellular carcinoma described as "pseudoadrenal mass" (patient 20) (G and H). The images are coronal sections through the midabdomen obtained between 25 and 45 min (^{11}C-metomidate) or 45 and 65 min (^{18}F-FDG) after injection. Tumor is indicated in each case by a white arrow, and normal adrenal, when visible in the same section, by a black arrow. All adrenocortical tumors (first 3 rows) have much higher uptake of ^{11}C-metomidate than of ^{18}F-FDG, whereas the opposite is true for the noncortical neoplasia shown in the lowest row. In this case (G), uptake of ^{11}C-metomidate is not confined to tumor but occurs in a rim of adrenal tissue (black arrow) displaced by the mass. Initially, the high ^{18}F-FDG uptake of the adenoma in 1 d was misjudged as metastasis, with an average SUV of 3.9 (maximum, 6). Liver has invariably high uptake of ^{11}C-metomidate, and tracer excreted in the urinary tract presents the highest radioactivity in ^{18}F-FDG images.

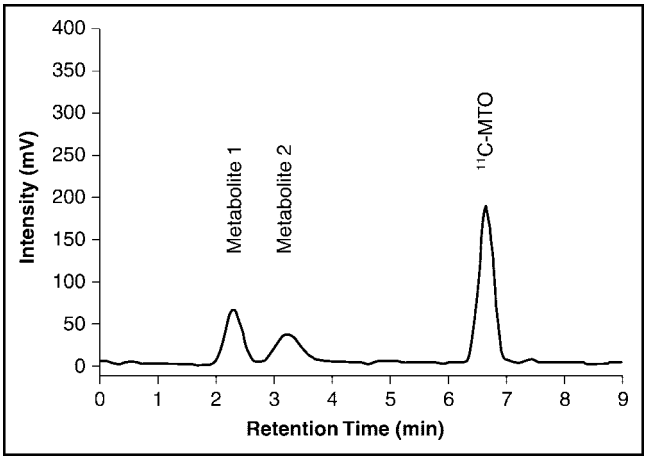

FIGURE 2. Representative HPLC chromatogram of a venous plasma sample at 6 min after tracer injection showing 3 peaks designated as metabolites 1 and 2 and native ^{11}C-metomidate (MTO). The retention times for peaks 1, 2, and 3 are 2.3, 3.2, and 6.6 min, respectively.

7), inactive adenomas (median SUV = 12.2; range, 7.8–25.4; n = 5), normal adrenals (median SUV = 9.4; range, 4.6–13.8; n = 20), pheochromocytomas (SUVs = 7.8 and 10.5; n = 2), and noncortical malignancies (SUVs = 2.0, 2.3, and 6.2; n = 3). The solitary lipoma had an average SUV of 13.3, and in the cyst a very low tracer uptake was seen, with an average SUV of 1.2, the lowest value among all (Fig. 4). True uptake of ^{11}C-metomidate into pheochromocytomas and lipoma may actually be lower, since the reported values are affected by the rim of displaced adrenal cortex surrounding the tumor (*10*).

The graphical K_i was highest for the adrenocortical carcinoma (1.14), followed by active adenomas (median K_i = 0.66; range, 0.33–0.78; n = 4), normal adrenal glands (median K_i = 0.37; range, 0.15–0.58; n = 12), and inactive adenomas (K_is = 0.24 and 0.37, n = 2). The median K_i for liver was 0.33 (range, 0.12–0.55; n = 11), and the respective SUV was 6.7 (range, 2.5–12.2; n = 21). A significant association between adenoma size and uptake of ^{11}C-metomidate could not be demonstrated with SUV or K_i as an index of tissue ^{11}C-metomidate metabolism.

Comparison of ^{11}C-Metomidate and ^{18}F-FDG

^{18}F-FDG was not helpful in distinguishing adrenal tumors, with the exception of 2 of the 3 noncortical malignancies, which had characteristically high glycolytic activity coupled with low uptake of ^{11}C-metomidate (Figs. 1G and 1H). Of interest was the relatively low uptake of ^{18}F-FDG in adrenocortical carcinoma (average SUV = 2.9 and maximum SUV = 3.8; Fig. 1F) and in bilateral adrenal metastases from renal cell cancer, which had low maximum SUVs of 2.4 and 2.3. The primary tumor in the right kidney had been previously embolized and was difficult to see in the vicinity of high ^{18}F-FDG activity excreted in the pelvis. Although ^{18}F-FDG was believed to generally be less informative than ^{11}C-metomidate, active adenomas (median SUV = 2.3; range, 1.8–3.9; n = 7) and the 2 pheochromocytomas (average SUVs = 3.0 and 2.9) showed higher uptake of ^{18}F-FDG than did the 3 inactive adenomas, with SUVs of 1.6, 1.7, and 1.7 (Figs. 1B and 1D). Again, no association between tracer uptake and mass size could be found.

To assess the relationship between adenoma metabolism and hormonal activity, ratios of tumor to normal adrenal were defined for ^{11}C-metomidate and ratios of tumor to liver, for ^{18}F-FDG. The ^{11}C-metomidate ratio could distinguish both active and inactive adrenocortical adenomas from other tumors (active vs. others, P = 0.003; inactive vs. others, P = 0.019) but was not different between hormon-

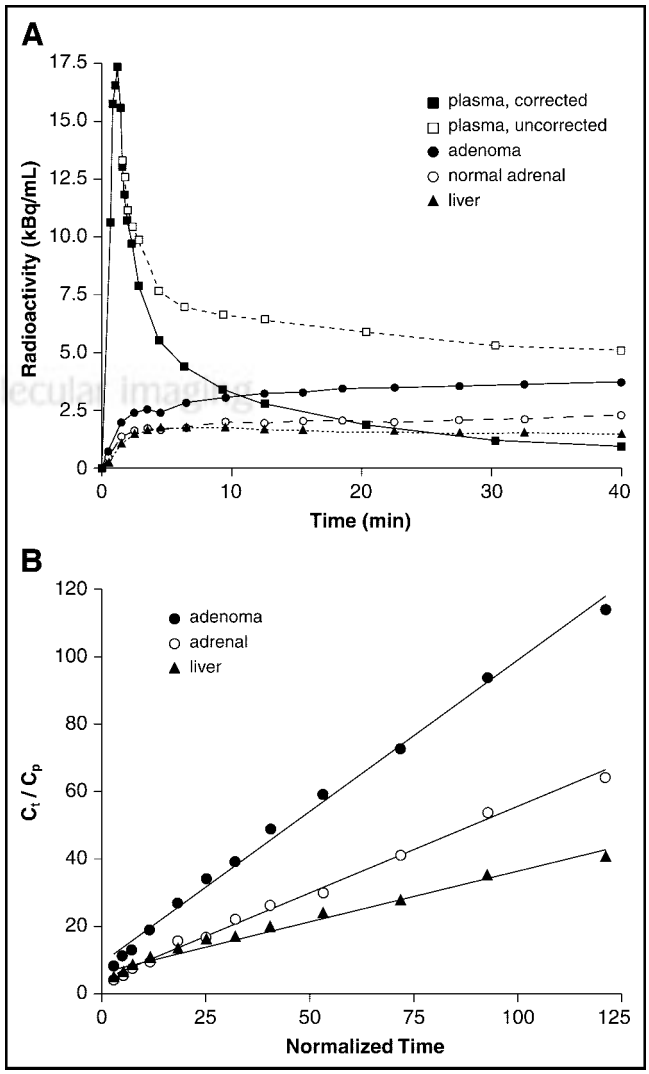

FIGURE 3. Time–activity curve for venous plasma and selected tissues (A) and Patlak graphical analysis for adenoma, normal adrenal, and liver (B) in a patient undergoing dynamic ^{11}C-metomidate PET. The high contribution of blood metabolites of ^{11}C-metomidate in the uncorrected plasma curve make it inappropriate for graphical analysis.

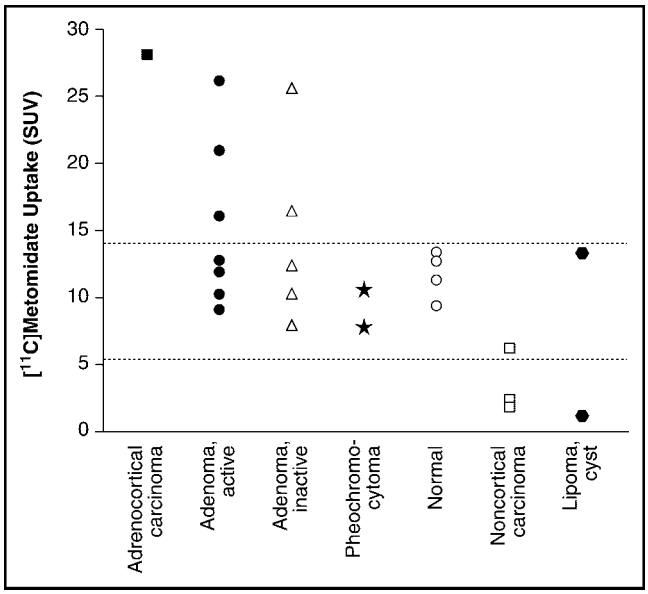

FIGURE 4. Average ^{11}C-metomidate SUV in incidentaloma. Dotted lines show variability within 12 normal adrenals, excluding a single exceptionally low value of 4.6. The SUV in lipoma was relatively high, most likely because of the contribution of normally functioning adrenal tissue.

ally active and inactive adenomas (Fig. 5). The ^{18}F-FDG ratio in noncortical tumors ($n = 7$) was not different from that in any other adrenal masses, including active and inactive adenomas ($n = 12$). This lack of significance depended strongly on the low number of malignant lesions and unexpectedly low uptake of ^{18}F-FDG in 2 of these 4 neoplasias.

DISCUSSION

Three major issues emerging from the discovery of adrenal incidentaloma are disclosure of malignancy, characterization of tissue type, and characterization of hormonal secretory activity. It is widely accepted that patients having abnormal hormonal screening results or adrenal masses greater than 3–4 cm in diameter should undergo surgery whereas patients with nonfunctioning tumors that show typical radiologic features suggesting benignity are candidates for follow-up and repeated imaging studies (*1,2*). In patients with benign normosecretory tumors, adrenalectomy may be associated with unjustified morbidity, and patients with adrenal metastasis, in turn, require systemic rather than localized treatment. Nuclear scintigraphy aids in proper management of incidentalomas by helping with discrimination between lesions derived from adrenal cortex and lesions derived from adrenal medulla (*8*), whereas ^{18}F-FDG PET has an established role in the diagnostic work-up of patients likely to have metastatic disease in the adrenals and other organs (*4,15*). Until now, radiolabeled cholesterol derivatives have been the first choice for γ-imaging of the adrenal cortex, whereas ^{123}I- or ^{131}I-labeled metaiodobenzylguanidine, a norepinephrine analog, is a common tracer for depicting tumors arising from the adrenal medulla (*8*). Because PET is now increasingly available in the clinical setting, pheochromocytomas may be diagnosed with ^{18}F-FDG (*16*) and ^{18}F-fluorodopa (*17*), and inhibitors of steroid biosynthesis, such as ^{11}C-metomidate, may become counterparts of ^{18}F-FDG and ^{18}F-fluorodopa for PET imaging of the adrenal cortex (*9,10*).

The current study was performed under European COST action B12, aiming to develop a noninvasive test for evaluation of adrenal incidentalomas with PET. We looked specifically at the uptake kinetics of ^{11}C-metomidate in tumors and normal adrenal glands and in liver and venous

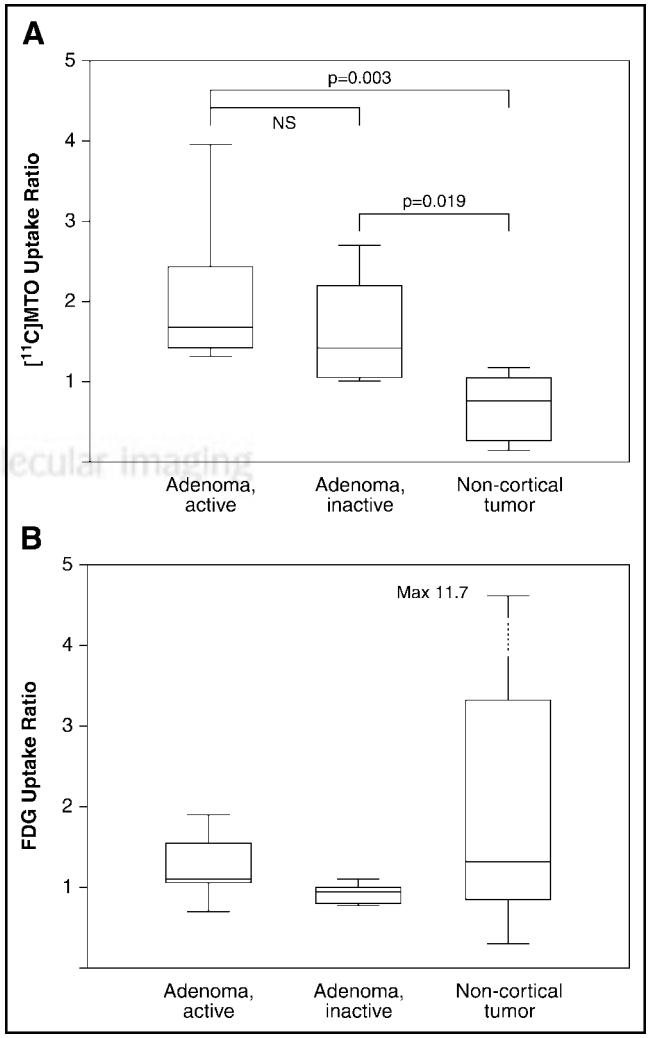

FIGURE 5. Box plots of SUV ratios for patients with active and inactive adenomas and noncortical tumors: tumor to normal adrenal for ^{11}C-metomidate (MTO) (A) and tumor to liver for ^{18}F-FDG (B). The error bars and lines within boxes represent the highest and lowest quartiles and the medians, respectively, of the data distribution. The ^{11}C-metomidate SUV ratio well distinguishes adenomas from other tumors, whereas ^{18}F-FDG shows clearly higher values for noncortical tumors. Because noncortical tumors have a very mixed character, they do not take up significantly more ^{18}F-FDG than do adenomas.

plasma and compared the findings with those on ^{18}F-FDG images obtained in steady state. In line with the preclinical validation study (*9*) and the first clinical study (*10*), we could demonstrate high uptake of ^{11}C-metomidate in adrenocortical tumors and normal adrenal glands as a sign of sustained 11β-hydroxylase activity. Decreased tracer uptake, in comparison with physiologic uptake, was seen in pheochromocytomas, cysts, and noncortical malignancies such as lymphoma and metastatic carcinomas, whereas adrenocortical carcinoma had the highest uptake of ^{11}C-metomidate among all lesions. ^{18}F-FDG was clearly inferior to ^{11}C-metomidate for depicting adrenal lesions if they were adenomas and, somewhat surprisingly, also in the solitary case of adrenocortical carcinoma. The low uptake of ^{18}F-FDG in adrenal metastases from renal cell cancer was less surprising because ^{18}F-FDG is known to have only a limited role in the diagnosis of renal cell carcinoma (*18*).

The uptake kinetics of ^{11}C-metomidate in adrenal tissue are favorable for PET imaging because irreversible binding of the tracer occurs over the first 45 min (Fig. 3). Because 2 large fractions of ^{11}C-metomidate metabolites occur in plasma, it is necessary to correct the plasma input function for these yet unidentified radiochemical species before applying graphical analysis to assess binding of ^{11}C-metomidate. This correction was successfully performed for 12 patients to calculate graphical influx constant K_i (Fig. 3), and in further analysis we showed that the obtained K_is could be replaced by the robust SUV approach commonly used in clinical oncology (*4,14*). K_i and SUV were not associated with mass size, and pheochromocytomas were seen to have the highest uptake in the outer rather than the inner zone of tumor—a finding compatible with the steroid-synthesizing property's being the major determinant of uptake of ^{11}C-metomidate in adrenal tissue (*9*). This does not translate, however, to a direct measure of rate of adrenocortical hormone synthesis, since the SUVs in active and inactive adenomas overlapped widely, in keeping with the findings of Bergström et al. (*10*). Furthermore, uptake ratios for adenoma to contralateral adrenal gland were not significantly different between active and nonsecretory adenomas (Fig. 5).

Although ^{11}C-metomidate PET does not immediately replace ^{131}I-labeled cholesterol derivatives in the functional evaluation of adrenal cortex, a search for new tracers applicable to positron imaging is in order with the widespread expansion of dedicated PET scanners. The major advantages of PET are rapid completion of the imaging, within 1 h, and a resolution and sensitivity better than those of adrenal scintigraphy. Clearly, the value of quantitative ^{11}C-metomidate PET will remain obscure until the results from the larger European multicenter study are at hand. In our trial, most patients were seen by a clinical endocrinologist; we hope that on that basis the multicenter trial included more patients with metastatic tumors and thus avoided the slight referral bias of the current study. Unfortunately, it seems difficult to distinguish adrenocortical adenoma from carcinoma with the current technique, but for a patient with known carcinoma, ^{11}C-metomidate should be a specific tracer for metastatic disease (*10*). For patients presenting with adrenal masses and a history or strong suggestion of neoplastic disease, ^{18}F-FDG PET may still be the study of choice because whole-body imaging may conceal other deposits of cancer in addition to adrenal metastasis (*15*).

CONCLUSION

We conclude that the pattern of ^{11}C-metomidate uptake facilitates discrimination between various types of adrenal masses, suggesting that ^{11}C-metomidate PET may be useful for functional evaluation of incidentalomas. The radiologic features of the adrenal mass, a clinical history addressing the risk for malignant disease, and the hormonal profile of the patient should be considered when assessing the advantages of ^{11}C-metomidate relative to those of other positron-emitting tracers such as ^{18}F-FDG and scintigraphic techniques using cholesterol derivatives or ^{123}I-metaiodobenzylguanidine. Further to be emphasized is that ^{11}C-metomidate PET, rather than representing a new modality to replace the established methods, remains complementary to CT and MRI in the diagnosis and management of incidentalomas.

ACKNOWLEDGMENTS

We are grateful to Professors Bengt Långström and Mats Bergström from Uppsala PET Centre, Sweden, for sharing their expertise in ^{11}C-metomidate imaging. The staffs of the Turku Cyclotron and the Radiochemistry Laboratory are thanked for technical support and advice, and the technologists at the PET Centre are thanked for excellent help in imaging the patients. This work was supported in part by European Union COST action B12 (http://cost.cordis.lu).

REFERENCES

1. Barzon L, Boscaro M. Diagnosis and management of adrenal incidentalomas. *J Urol.* 2000;163:398–407.
2. Bertherat J, Mosnier-Pudar H, Bertagna X. Adrenal incidentalomas. *Curr Opin Oncol.* 2002;14:58–63.
3. Lam KY, Lo CY. Metastatic tumours of the adrenal glands: a 30-year experience in a teaching hospital. *Clin Endocrinol.* 2002;56:95–101.
4. Boland GW, Goldberg MA, Lee MJ, et al. Indeterminate adrenal mass in patients with cancer: evaluation at PET with 2-[F-18]-fluoro-2-deoxy-D-glucose. *Radiology.* 1995;194:131–134.
5. Mantero F, Terzolo M, Arnaldi G, et al. A survey on adrenal incidentaloma in Italy. *J Clin Endocrinol Metab.* 2000;85:637–644.
6. Bulow B, Ahren B. Adrenal incidentaloma: experience of a standardized diagnostic programme in the Swedish prospective study. The Swedish Research Council Study Group of Endocrine Abdominal Tumours. *J Intern Med.* 2002; 252:239–246.
7. Korobrin M. CT characterization of adrenal masses: the time has come. *Radiology.* 2000;217:629–632.
8. Rubello D, Bui C, Casara D, Gross MD, Fig LM, Shapiro B. Functional scintigraphy of the adrenal gland. *Eur J Endocrinol.* 2002;147:13–28.
9. Bergström M, Bonasera TA, Lu L, et al. In vitro and in vivo primate evaluation of carbon-11-etomidate and carbon-11-metomidate as potential tracers for PET imaging of the adrenal cortex and its tumors. *J Nucl Med.* 1998;39:982–989.

10. Bergström M, Juhlin C, Bonasera TA, et al. PET imaging of adrenal cortical tumors with the 11β-hydroxylase tracer ^{11}C-metomidate. *J Nucl Med.* 2000;41: 275–282.
11. Någren K, Halldin C. Methylation of amide and thiol functions with [^{11}C]methyl triflate, exemplified by [^{11}C]NMSP, [^{11}C]flumazenil and [^{11}C]methionine. *J Labelled Compds Radiopharm.* 1998;41:831–841.
12. Hamacher K, Coenen HH, Stocklin G. Efficient stereospecific synthesis of no-carrier-added 2-[^{18}F]-fluoro-2-deoxy-D-glucose using aminopolyether supported nucleophilic substitution. *J Nucl Med.* 1986;27:235–238.
13. Patlak CS, Blasberg RG, Fenstermacher JD. Graphical evaluation of blood-to-brain transfer constants from multiple-time uptake data. *J Cereb Blood Flow Metab.* 1983;3:1–7.
14. Minn H, Leskinen-Kallio S, Lindholm P, et al. [^{18}F]Fluorodeoxyglucose uptake in tumors: kinetic vs. steady-state methods with reference to plasma insulin. *J Comput Assist Tomogr.* 1993;17:115–123.
15. Yun M, Kim W, Alnafisi N, Lacorte L, Jang S, Alavi A. ^{18}F-FDG PET in characterizing adrenal lesions detected on CT or MRI. *J Nucl Med.* 2001;42:1795–1799.
16. Shulkin BL, Thompson NW, Shapiro B, Francis IR, Sisson JC. Pheochromocytomas: imaging with 2-[fluorine-18]fluoro-2-deoxy-D-glucose PET. *Radiology.* 1999;212:35–41.
17. Hoegerle S, Nitzsche E, Altehoefer C, et al. Pheochromocytomas: detection with ^{18}F DOPA whole body PET—initial results. *Radiology.* 2002;222:507–512.
18. Miyakita H, Tokunaga M, Onda H, et al. Significance of ^{18}F-fluorodeoxyglucose positron emission tomography (FDG-PET) for detection of renal cell carcinoma and immunohistochemical glucose transporter 1 (GLUT-1) expression in the cancer. *Int J Urol.* 2002;9:15–18.